

Reemission of inorganic pollution from permafrost? – a freshwater hydrochemistry study in the lower Kolyma basin (North-East Siberia)

Danuta Szumińska¹, Krystyna Koziol¹, Sergiej R. Chalov¹, Vasilii A. Efimov², Marcin Frankowski³, Sara Lehmann-Konera⁴, and Zaneta Polkowska⁵

¹Uniwersytet Kazimierza Wielkiego w Bydgoszczy Instytut Geografii

²Moskovskij gosudarstvennyj universitet imeni M V Lomonosova

³Uniwersytet im Adama Mickiewicza w Poznaniu Wydział Chemii

⁴Uniwersytet Marii Curie-Skłodowskiej w Lublinie Wydział Nauk o Ziemi i Gospodarki Przestrzennej

⁵Politechnika Gdanska Wydział Chemiczny

December 20, 2022

Abstract

Permafrost regions are under particular pressure from climate change resulting in widespread landscape changes, which impact also freshwater chemistry. We investigated a snapshot of hydrochemistry in various freshwater environments in the lower Kolyma river basin (North-East Siberia, continuous permafrost zone) to explore the mobility of metals, metalloids and non-metals resulting from permafrost thaw. Particular attention was focused on heavy metals as contaminants potentially released from the secondary source in the permafrozen Yedoma complex. Permafrost creeks represented the Mg-Ca-Na-HCO₃-Cl-SO₄ ionic water type (with mineralisation in the range 600-800 mg/L), while permafrost ice and thermokarst lake waters were the HCO₃-Ca-Mg type. Multiple heavy metals (As, Cu, Co, Mn and Ni) showed much higher dissolved phase concentrations in permafrost creeks and ice than in Kolyma and its tributaries, and only in the permafrost samples and one Kolyma tributary have we detected dissolved Ti or Hg. In thermokarst lakes, several metal and metalloid dissolved concentrations increased with water depth (Fe, Mn, Ni and Zn - in both lakes; Al, Cu, K, Sb, Sr and Pb in either lake), reaching 1370 µg/L Cu, 4610 µg/L Mn, and 687 µg/L Zn in the bottom water layers. Permafrost-related waters were also enriched in dissolved phosphorus (up to 512 µg/L in Yedoma-fed creeks). The impact of permafrost thaw on river and lake water chemistry is a complex problem which needs to be considered both in the context of legacy permafrost shrinkage and the interference of the deepening active layer with newly deposited anthropogenic contaminants.

1. INTRODUCTION

Permafrost loss has been observed widely in the Northern Hemisphere since the second half of 20th century (Streletskiy *et al.*, 2015) and it has impacted markedly both terrestrial and aquatic environments (Mann *et al.*, 2022; Vonk *et al.*, 2015). Further significant changes are predicted in permafrost environments during the 21st century (Smith *et al.*, 2022; Streletskiy *et al.*, 2021; Teufel & Sushama, 2019) as the climate warms (Overland J., 2017; Overland *et al.*, 2014). Such changes will be both vertical and horizontal, resulting in deeper active layers (Abramov *et al.*, 2021), shrinking permafrost extent, and the retreat of its respective zones (Lim *et al.*, 2019; Streletskiy, 2021). The progressing permafrost degradation leads to important and lasting changes in geomorphological processes (Rudy *et al.*, 2017; Tananaev & Lotsari, 2022), hydrological phenomena (Rudy *et al.*, 2017; Suzuki *et al.*, 2021) and biogeochemical cycles (Grosse *et al.*, 2016; Mann *et al.*, 2012; Vonk *et al.*, 2015).

Hydrochemical changes in permafrost regions are increasingly probable, leading to both temporary and permanent hazards to the surface water quality in the Arctic (Brubaker *et al.* , 2012; Gunnarsdóttiret al. , 2019). Permafrost active layer deepening and the formation of new thermokarst lakes, taliks and drainage pathways (Dzhamalov & Safronova, 2018; in't Zandt *et al.* , 2020; Tananaev & Lotsari, 2022) all lead to changes in the migration of chemical compounds (Frey & McClelland, 2009; Monhonval *et al.* , 2021) both horizontally and vertically (Ji *et al.* , 2021; Tananaev *et al.* , 2021). The newly formed drainage pathways may leach chemical compounds from layers previously disconnected from groundwater flow (Jiet al. , 2021; Lim *et al.* , 2019). Thermoerosion phenomena lead to intense erosion and thaw slump formation. Such phenomena impact the fluvial transport of suspended sediment and chemical compounds along the main hydrological pathways, to the estuaries and the ocean (Chalovet al. , 2018; Frey & McClelland, 2009; Kokelj *et al.* , 2013; Toohey *et al.* , 2016). Both natural and antropogenic chemical compounds may become mobilised from permafrost into surface waters (Kosek *et al.* , 2019; Lehmann-Konera *et al.* , 2018), and the antropogenic compounds may be of both local and long-range-transport origin (Potapowicz *et al.* , 2019; Szopińskaet al. , 2016).

The studies on the hydrochemical impacts of climate change in Siberian Arctic rivers have focused mainly on the organic carbon (OC) transport, including the dissolved OC (DOC), suspended particulate OC (POC) and riverbed sediment OC (SOC) (e.g., Holmes *et al.* , 2012; Jonget al. , 2022; Mann *et al.* , 2012; Wild *et al.* , 2019). Compared to the research on OC, the recognition of inorganic elements transport, including heavy metals, is relatively poor and limited to selected elements (Ji *et al.* , 2021; Kuchmenko *et al.* , 2002; Lim *et al.* , 2019). Systematic research on the potential accumulation of heavy metals in permafrost has only been conducted on mercury (Wang *et al.* , 2022). Therefore, we present a study on the possible release of contaminants from permafrost into freshwater. Our objective was to perform a detailed hydrochemical assessment of permafrost thaw impact on the inorganic chemicals occurrence in the lower Kolyma River basin. We investigate this question in various freshwater environments: thermokarst lakes, permafrost ice, permafrost thaw creeks, and in watercourses representing various proportions of permafrost thaw supply.

2. METHODS

2.1. Study area and sampling

The study region is located in the lower Kolyma watershed (Figure 1) in a transitional zone between boreal forest (northern taiga) in the south and tundra ecosystems in the northern Yakutia. Kolyma is one of the largest pan-Arctic watersheds with a total area of 653,000 km², a total river length of 2,129 km, and annual water discharge of 109 ± 7 km³ (Holmes *et al.* , 2012), fully underlined by continuous permafrost (Mann *et al.* , 2012). The Arctic coastal lowlands of northeastern Yakutia constitute vast accumulative plains formed mostly by the Late Pleistocene loess-like Yedoma Ice Complex, characterized by a high ice and organic matter content (Abramov *et al.* , 2021). Permafrost thickness in the area reached 500-600 m, and mean annual ground temperatures (MAGT) before the 1990s were of -8 to -11degC within the tundra and -7degC to -8degC in the taiga (Yershov *et al.* , 1991). The very high ice content (up to 95% by volume) of Yedoma deposits in the Kolyma lowland (Strausset al. , 2021) makes them extremely vulnerable to climate warming. In 2000-2016 (Ran *et al.* , 2022), MAGT in the studied region increased significantly against the former century due to climate warming, and now ranged from -8degC to -4degC. Mean annual air temperature (MAAT) in Cherskii (68.75degN, 161.28degE, 28 m asl) increased from -12 degC in the 1960s to -10 degC in the 2000s, with a positive trend of 0.0472 degC per year (Sakai *et al.* , 2016).

MAAT in Cherskii in the year of sampling (2021) amounted to -9.8degC and was lower than the MAAT in the years 2006-2021 (-8.9degC) (*Suppl. Mat. 1, Table S2*). However, the maximum air temperature in 2021 was the highest in the years 2006-2021 ($t_{\max} = 33.4$ degC) and it occurred directly before our sampling (*Suppl. Mat. 1, Table S2 ,Figure S1*). In the study area, the minimum air temperature ranged from -40.2degC to -49.7degC and in 2006-2021 was observed in January, February or December. The maximum air temperature was observed in June-August, ranging 25.9degC – 33.4degC (*Suppl. Mat. 1, Table S2*). The mean monthly air temperature was higher than 0degC from May to September (in 2006-2021) (*Suppl. Mat. 1, Figure S2*).

Samples have been collected between 19th and 22nd July 2001 (28 in total). River waters were collected in the four cross sections of Kolyma (Cherskii, samples K11-K13; Yermolovo, K21-K23; Duvanny Yar, K31-K33, K31b-K33b; Kolymskoye, K4), and in the mouth sections of the Anyui (A1, A2) and Omolon (O1) tributaries. In addition, a meltwater creek and ice were sampled from a permafrost cliff located at Duvanny Yar (P1-P3), and lake waters were collected from two thermokarst lakes (L11-L15, L21-L24) (Figure 1, a detailed description in *Suppl. Mat. 1, Table S1*). The Kolyma river samples were taken at the middle depth of three vertical profiles in the channel cross sections, except of Kolyma upstream of the permafrost cliff, where only one sample (from the middle of the channel) was collected. Water samples were pumped out with a filterless submersible 12V pump (details in Chalov *et al.* , 2022). In both lakes, samples were taken along a vertical profile located above the deepest point of the lake. Among the sample sites, direct permafrost influence was expected at the permafrost cliff, in Lakes 1 and 2 and in Kolyma cross section K3 (directly below permafrost cliff).

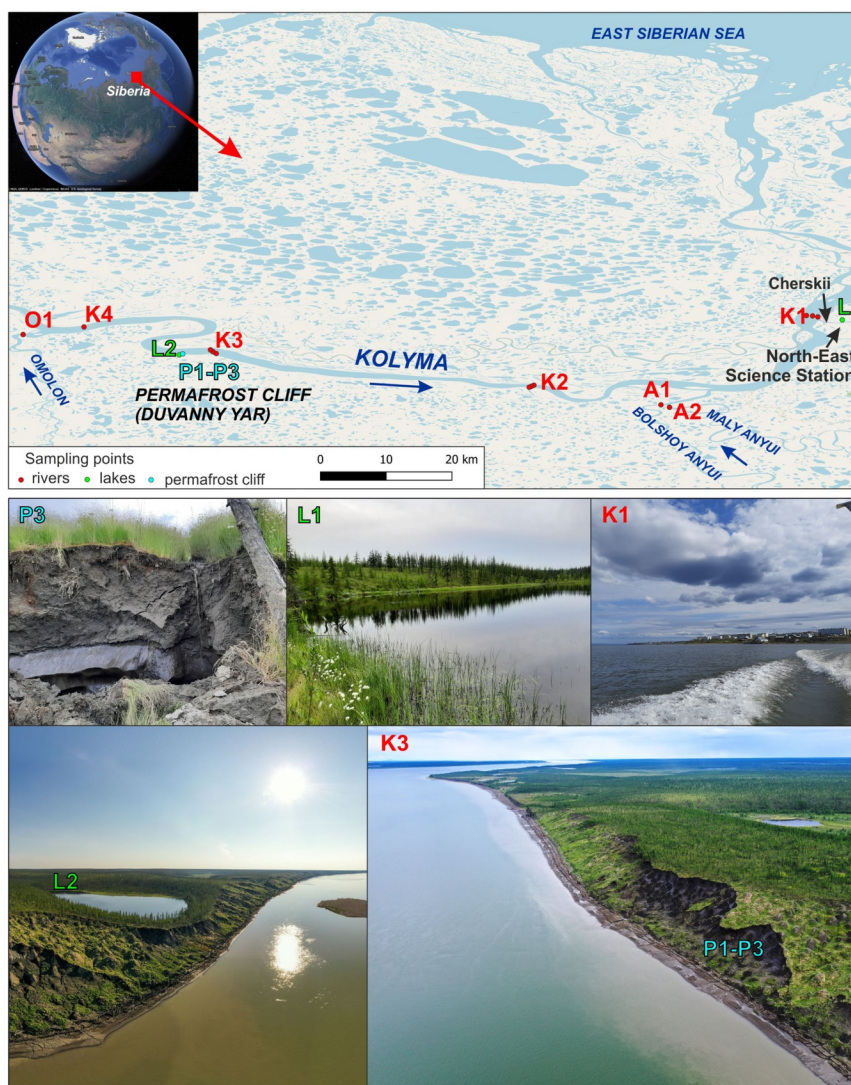


Figure 1. Location of the study area and sampling sites. Please note that all K-symbol samples come from Kolyma river cross sections.

2.2. Analytical methods

All water samples, due to their turbidity, were filtered through 0.7- μm -pore-size glass fiber filters (Whatman GFF, pre-combusted in 400°C, 24 h).. Samples were kept in cool storage (+4°C) and analysed approximately two months since collection time. Specific electric conductivity (SpC), pH and dissolved oxygen were measured in the field with a multiparameter YSI Pro Plus probe with a 4-sport Quattro Cable (11m).

Dissolved organic carbon (DOC) was determined through a total organic carbon (TOC) measurement in filtrate with a TOC-VCSH/CSN analyser (Shimadzu; the method of catalytic oxidation with oxygen at 680°C and nondispersive infrared spectroscopy detection). Calibration was performed with a potassium phthalate standard (Shimadzu), with an $R^2 = 0.998$. CVs of five sample replicates were below 2%. Samples with DOC concentrations above the analytical range were diluted with MilliQ water (Merck Life Sciences). Only a few samples with a high suspended sediment content were analysed for POC (details in *Suppl. Mat. 1*).

Major ions (F^- , Cl^- , NO_2^- , Br^- , NO_3^- , PO_4^{3-} , SO_4^{2-} , Na^+ , NH_4^+ , K^+ , Ca^{2+} and Mg^{2+}) were determined using Dionex ICS 3000 (Dionex, USA), calibrated with dilutions of a 1000 mg L^{-1} single-ion standard solutions. Analytical accuracy was checked with the TraceCERT® Multi Anion Standard 1 for IC (69734-100ML) and Multi Cation Standard 1 for IC (91286-100ML) (all solutions by Merck Life Science).

Elemental analysis was performed in acidified (with high-purity nitric acid, Suprapur, Merck Life Science) filtrate using inductively coupled plasma optical emission spectrometry (ICP-OES 9820, Shimadzu, Japan) for Be, P, S and Ti. Inductively coupled plasma mass spectrometry (ICP-MS 2030, Shimadzu, Japan) was applied for Ag, Al, As, Ba, Bi, Cd, Co, Cr, Cu, Fe, Hg, Li, Mn, Mo, Ni, Pb, Sb, Se, Si, Sr, V and Zn. For calibration of the ICP-MS, the ICP IV multielement standard (Merck Life Sciences) and single-element standards of As, Be, Sb, Se, Mo, and V (Sigma-Aldrich, USA) were used. Single-element 1000 mg L^{-1} standards (Sigma-Aldrich, USA) were applied for the ICP-OES. Internal standards controlling for the MS signal were solutions of Sc, Rh, Tb, and Ge in suprapure 1% HNO_3 (Merck). Accuracy of the analysis was checked with Sigma-Aldrich CRMs (certified reference materials) Trace Metals ICP-Sample 1 and Trace Metals ICP-Sample 2, with 98-104% recoveries. High-concentration samples were diluted with Milli-Q water (Direct 8 Purification System Water, Merck Life Sciences, France). All metals, non-metals and metalloids concentrations measured have been corrected for a procedural blank value if it exceeded the method limit of quantification (LOQ); in all other determinations, the blank correction was not required. The details of all measurement conditions and QA/QC parameters, including method LOQ, are given in the Supplementary material (*Suppl. Mat. 1, Table S3*).

2.3. Statistical methods

Cluster analysis was performed using Statistica version 13 (TIBCO Software Inc.) on a selection of variables listing elemental, ionic and DOC concentrations , with the selection criterion that only variables with 33% or fewer values < LOQ (or below blank) were taken into account to avoid artifacts in grouping. Prior to cluster analysis, values <LOQ (or below blank) were replaced by half LOQ (or blank, whichever was higher). All data was standardised (z-transformed) within variables. Clustering was performed using Ward's method and squared Euclidean distance. This analysis may be cross-compared with the principal component analysis presented in *Suppl. Mat. 1* .

Enrichment factors (EFs) relative to average concentration of elements in the suspended sediment of World rivers (after Viers *et al.* , 2009 and Taylor, 1964) have also been calculated and are shown in Table S4 (*Suppl. Mat. 1*).

3. RESULTS

3.1. Electric conductivity, pH and dissolved organic carbon (DOC)

SpC in the collected samples exhibited a wide range of values, from <50 $\mu\text{S cm}^{-1}$ in Lake 2 to 1405 $\mu\text{S cm}^{-1}$ in a sample from permafrost-fed creek P2 (*Suppl. Mat. 2*). Conductivities in the Kolyma water ranged 125-165 $\mu\text{S cm}^{-1}$, and 65-69 $\mu\text{S cm}^{-1}$ in its tributaries Anyui and Omolon. Finally, both Lakes 1 and 2 showed

SpCs $<100 \mu\text{S cm}^{-1}$, except the bottom layers of Lake 1 with a steep incline in SpC values, reaching $318 \mu\text{S cm}^{-1}$ near the bottom. Both lakes were thermally stratified, with much cooler water near the bottom (especially Lake 1, changing from $15\text{-}16^\circ\text{C}$ at the surface to $\sim 5^\circ\text{C}$ near the bottom). The bottom layers of Lake 1 were also strongly depleted in oxygen, which was confirmed by the precipitation of iron hydroxide in the collected samples, and infused with methane (Stepanenko *et al.*, 2011; Walter *et al.*, 2006).

Dissolved organic carbon (DOC) concentration showed consistent values within each one sample type, while it differed widely between the various water bodies. Particularly high DOC concentrations (max = 127 mg/L) were found in the permafrost-fed creeks at Duvanny Yar (Figure 2).

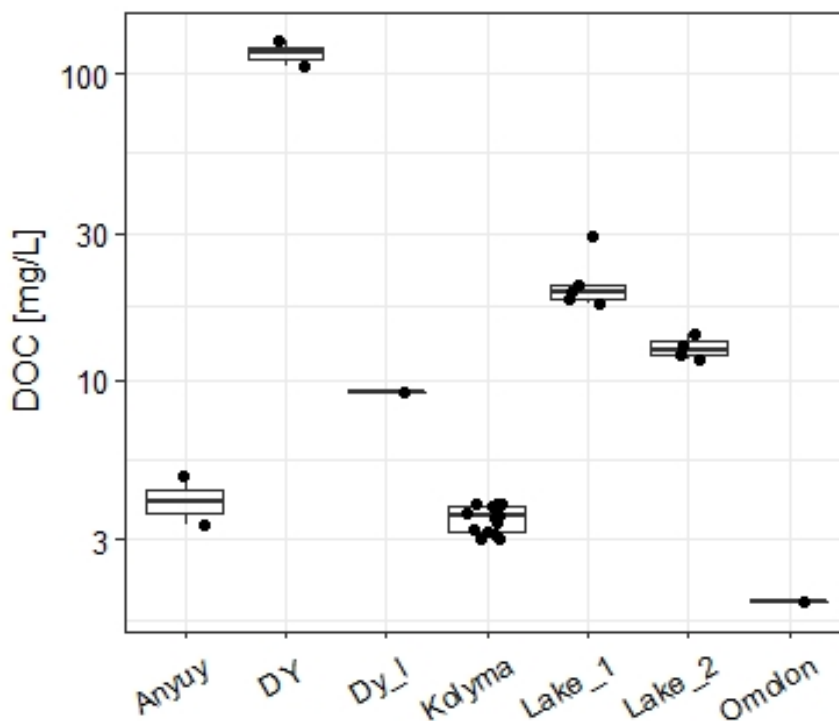


Figure 2. A DOC concentration boxplot grouped by the water bodies sampled: Anyuy, Kolyma and Omolon are river names; DY = permafrost-fed creeks draining a Yedoma cliff at Duvanny Yar; Dy_I – ice collected from Yedoma at the same site; Lake_1 = the thermokarst lake close to Cherskii.; Lake_2 = a thermokarst lake at Duvanny Yar. Please note the logarithmic scale of DOC concentration .

3.2. Major ions

Chloride and sulphate were the predominant anions in sampled waters (and presumably also bicarbonate, which was not measured, yet its concentrations estimated from the ionic balance approximated the concentrations of calcium ions, and if recalculated to mass, they were the main ions in the collected samples, reaching 311 mg L^{-1} in P2). Phosphate, nitrate, nitrite and bromide have only been detected in a few samples each, therefore they are not presented in graphs (Figure 3). The highest dissolved solid concentrations have been found in Yedoma-fed creeks ($>100 \text{ mg/L}$ of chloride and sulphate both), and sulphate was relatively high in most Kolyma river samples. Among cations, calcium was predominant, at the average level of 12.4 mg L^{-1} in the Kolyma river, while magnesium was usually second, exceeding Ca^{2+} only in P2 sample at 74.2 mg L^{-1} in the permafrost cliff creeks (DY; Figure 4). Permafrost-fed creeks exhibited relatively high concentrations (approx. 50 mg L^{-1} or more) of all three cations: Ca^{2+} , Mg^{2+} and Na^+ (Figure 4). If the ionic water type is defined, using the [mval] concentrations of major ions amounting to at least 20% of the anion

or cation total (*Suppl. Mat. 2*), three groups of objects emerge: (1) thermokarst lakes and permafrost ice represented the $\text{HCO}_3\text{-Ca-Mg}$ water type; (2) in the rivers, water types varied between $\text{SO}_4\text{-HCO}_3\text{-Ca-Mg}$, $\text{Ca-Mg-HCO}_3\text{-SO}_4$ and $\text{Ca-Mg-Na-HCO}_3\text{-SO}_4$, except sample A2 ($\text{SO}_4\text{-Ca-Mg}$); (3) permafrost creeks were of $\text{Mg-Ca-Na-HCO}_3\text{-Cl-SO}_4$ type.

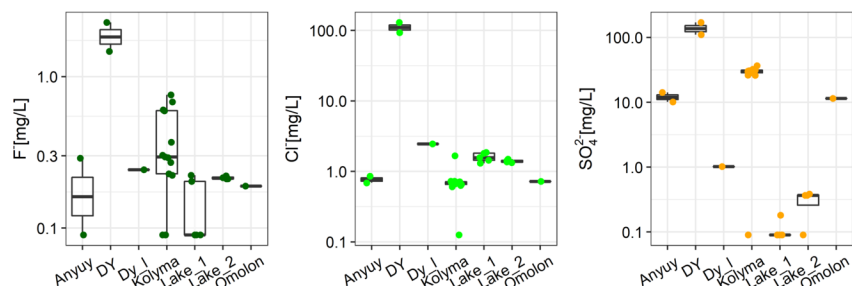


Figure 3. Major anions in the Kolyma region freshwaters. Nitrite, nitrate, bromide and phosphate, detected only in a few samples, are not shown. See *Suppl.mat. 2* for a full data table and Figure 2 caption for site symbols.

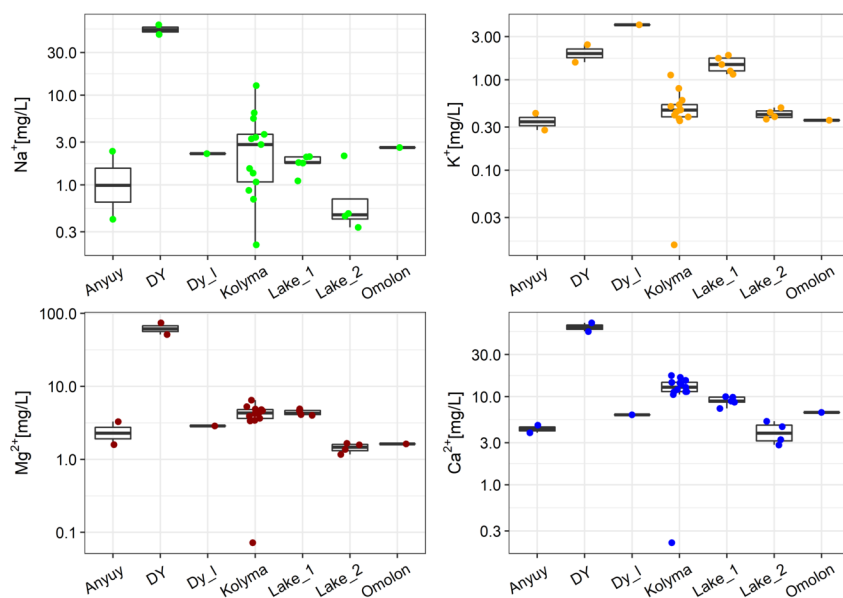


Figure 4. Major cations concentrations in freshwater samples from the lower Kolyma basin. Sampling sites named as in Figure 2.

3.3. Metals, metalloids and non-metals

Elemental concentrations exhibited a large variability (Figure 5), with maxima typically found in P1-P2 (Duvanny Yar) samples (Be, Co, Sb, Se, Sr, V), in the lower layers of lake waters (As, Cd, Cu, Fe, Mn, Ni, Si, Zn) or in single samples from Kolyma river (Ba, Li, Mo). Only Al showed the highest concentration in permafrost ice (sample P3). Multiple heavy metals showed much higher concentrations in permafrost creeks and ice (As $1.24\text{-}4.23 \mu\text{g L}^{-1}$, Cu $1.82\text{-}11.4 \mu\text{g L}^{-1}$, Co $0.57\text{-}3.99 \mu\text{g L}^{-1}$, Mn $122\text{-}1300 \mu\text{g/L}$, $\mu\text{g L}^{-1}\text{Ni}$ $3.36\text{-}16.5 \mu\text{g L}^{-1}$) than in Kolyma and its tributaries (As $0.22\text{-}0.81 \mu\text{g L}^{-1}$, Cu $0.70\text{-}5.72 \mu\text{g L}^{-1}$, Co $0.01\text{-}0.05 \mu\text{g L}^{-1}$,

Mn 0.61-14.1 $\mu\text{g L}^{-1}$, Ni 0.2-1.87 $\mu\text{g L}^{-1}$ (*Suppl. Mat. 2*). Permafrost samples also contained metals that were not typically found in other samples: Ti (15.7-30.3 $\mu\text{g L}^{-1}$) and Hg (0.128-0.131 $\mu\text{g L}^{-1}$). In the lakes, several metals concentrations increased with water depth: Fe, Mn, Ni and Zn concentrations did so in both lakes; Al, K, Sr in Lake 1, and Cu, Pb, Sb in Lake 2. The only instances of an opposite direction of change were Mo, Na and Sb in Lake 1. The highest concentrations of selected elements in this study were observed in lake bottom waters, e.g. $[\text{Cu}] = 1370 \mu\text{g/L}$, $[\text{Mn}] = 4610 \mu\text{g/L}$, and $[\text{Zn}] = 687 \mu\text{g/L}$. Bottom lake waters, permafrost creeks and ice were also enriched with phosphorus (up to 34.7 $\mu\text{g/L}$ in Lake 2, up to 512 $\mu\text{g/L}$ in creeks and 43.3 $\mu\text{g/L}$ in ice) (*Suppl. Mat. 2*).

Enrichment factors (EF) of all the collected samples indicate significant or higher enrichment in heavy metals (As, Cd, Co, Cu, Mn, Ni, Pb and Zn). The highest EFs in the dataset were found in lake bottom waters for As, Co, Cu, Mn, Ni, Pb and Zn (*Suppl. Mat. 1, Table S4*). Noteworthy is also the extremely high enrichment of the permafrost ice and creeks, as well as Maly Anyui (A2) sample in Hg. Furthermore, the concentration level of Cd was higher in the collected samples connected to permafrost than elsewhere: in permafrost creeks, permafrost ice, lower layers of lake water and in a few samples from the Kolyma river in the K3 cross section. In that particular cross section, the enrichment in Cd was higher in the mid-stream (samples K31 and K32) than in the river bottom waters (K31b, K32b), testifying to the limited mixing of dissolved elements in the vertical profile of the river, suggesting their local supply.

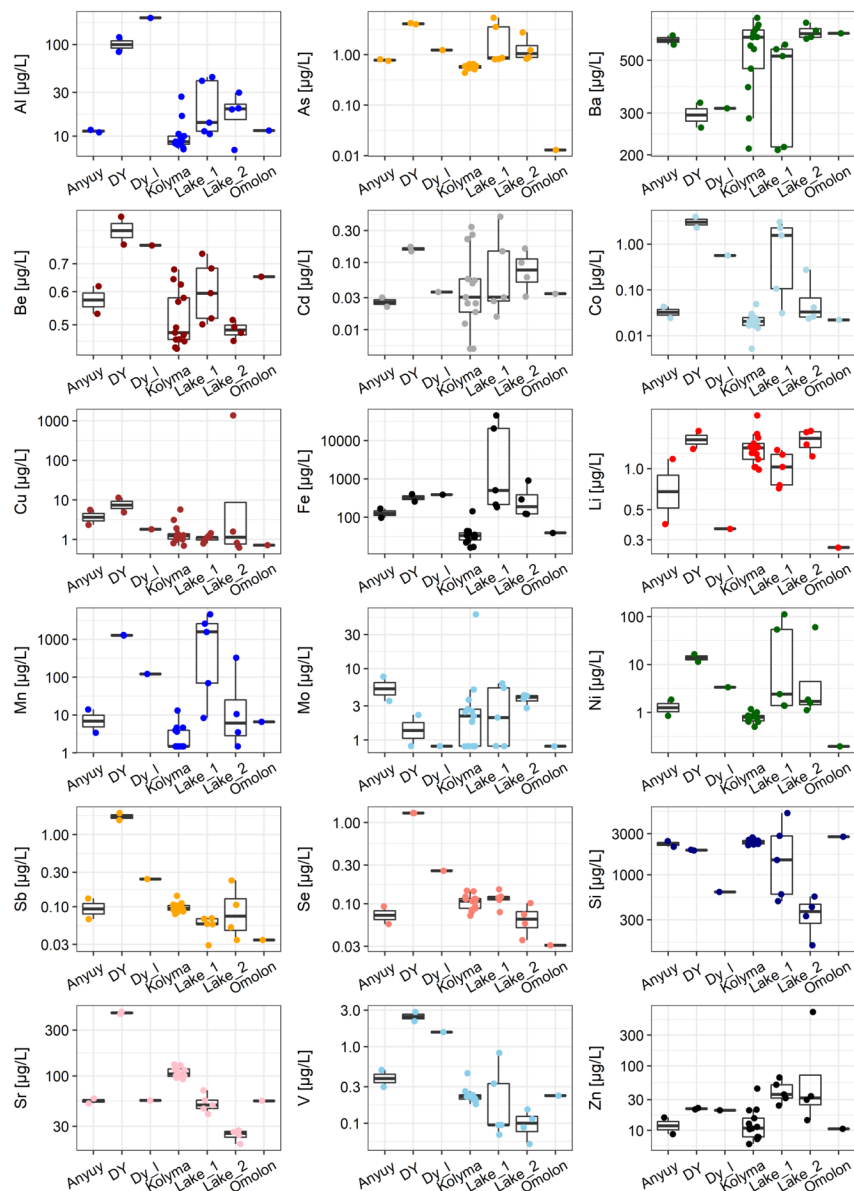


Figure 5. Elemental concentrations in the collected samples. Note the logarithmic scale of concentrations. Boxplots show quartiles and full range without outliers, points show all data. Sampling sites marked as in Figure 2.

3.4. Cluster analysis

To explore the patterns in elemental and ionic constituent concentrations, together with DOC, we performed cluster analysis. Grouping variables (Figure 6a), at the 33% maximum distance level, yielded 5 clusters: C1 (Zn & Cu), C2 (Mo, Li, Cd & Ba), C3 (Si, Ni, Mn & Fe), C4 (Be, Co, As, Al and K^+), and C5 (V, DOC, Se, Sb, Sr and all other ions). At the 67% level, C1 and C2 form one cluster together, and another is formed by C3 and C4, joined. Grouping samples (Figure 6b), on the other hand, resulted in three distinct clusters at the 33% maximum distance level: P1 & P2; L14 & L15; and all other samples. Notably, permafrost ice P3

was classified as relatively similar to the samples from the bottom of Lake 2 and one Kolyma river sample (K31). The variables distinguishing Lake 2 and the P3 ice from other samples were the concentrations of DOC, Al, Co, As, Mn, Ni, Fe, Zn, while the variables setting the permafrost creeks P1 and P2 apart were the concentrations of Si, Sr, Sb, V and the ions Na^+ , Mg^{2+} , F^- , and SO_4^{2-} (cf. *Figures S3 & S4, Suppl. Mat. 1*).

An additional cluster analysis (Figure 7), performed for river waters alone (Kolyma, Omolon and Anyui), yielded three clusters at 67% maximum distance level. Cluster c1 contained rock-derived elements, organics and some more typically anthropogenic contaminants (Si, Mn, Fe, Zn, Sb, Cu, V, Co, As, Ni and DOC); c2 grouped Li, Mo, Cd, Ba, Be, Al and Sr; and c3 joined Sr, Se, and all inorganic ions. Around 33% maximum distance, the c1 cluster divided into c1a (Si, Mn & Fe) and c1b (Zn, Sb, Cu, V, Co, As, Ni and DOC); cluster c2 consisted of c2a (Li, Mo & Cd) and c2b (Ba, Be & Al); and cluster c3 was composed also of two sub-clusters: c3a (Sr, Se, K^+ , Mg^{2+} , Ca^{2+} & SO_4^{2-}) and the saline c3b (Cl^- , Na^+ and F^-).

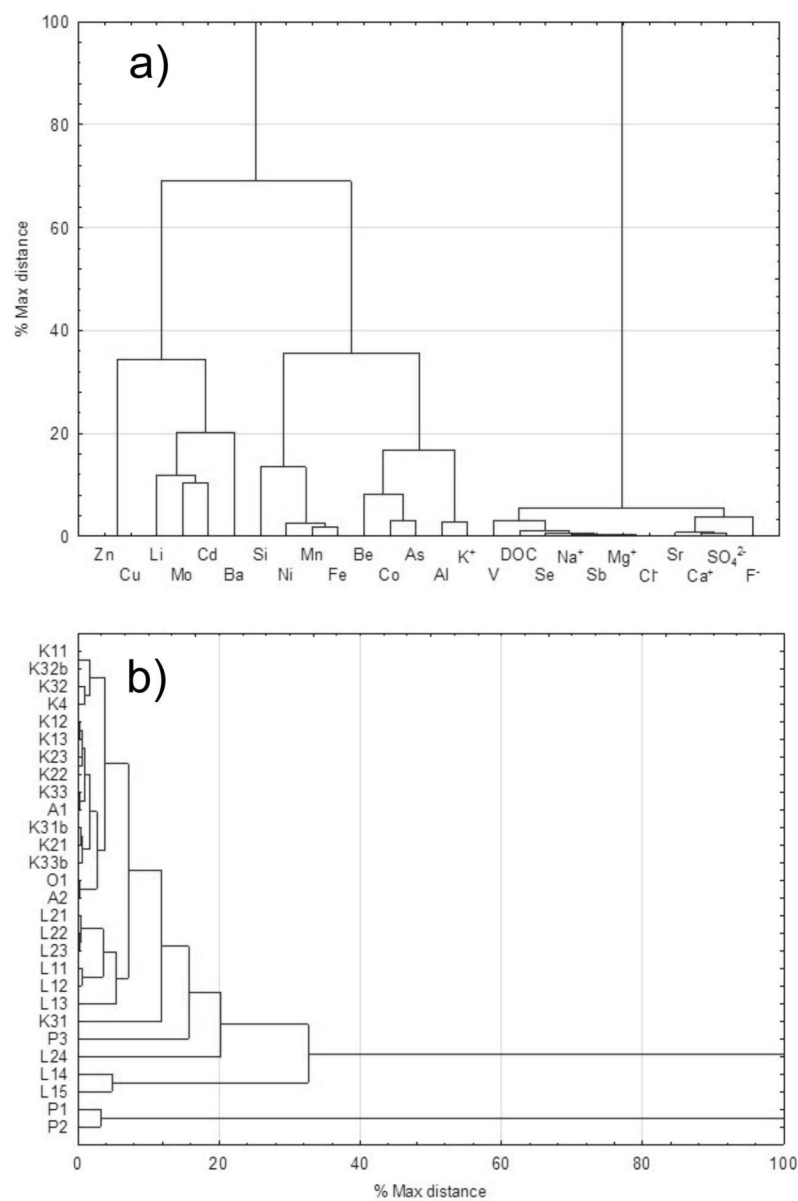


Figure 6. Cluster analysis results for all collected samples: a.) clustering variables; b.) grouping samples (objects).

Figure 7. Results of the cluster analysis performed on river samples data alone (Kolyma, Anyui and Omolon).

4. DISCUSSION

Permafrost regions have experienced dynamic environmental changes induced by climate change, especially in the north-eastern Siberia (Nitzbon *et al.* , 2020). Recent climate-induced increases in thaw propagation have triggered changes in local relief in the Yedoma uplands, including soil subsidence (Günther *et al.* , 2015), activation of thermokarst and thermoerosion processes (Grigoriev *et al.* , 2009; Morgenstern *et al.* ,

2021), and the expansion of pond and thermokarst lake areas (Nitze *et al.* , 2017; Veremeeva *et al.* , 2021). In the large rivers, an increase in runoff is both expected and already observed: in the Kolyma, mean annual discharge has increased over the 2010–2020 by 27.7% (94.6 to 120.7 km³ year⁻¹) compared to a baseline period of 1971–2000 (Mann *et al.* , 2022). The same authors estimated an increase of 50% ($\pm 25\%$) in Kolyma’s mean annual runoff by 2100, in line with climate projections. Climate warming resulted also in an increase in Kolyma’s sediment transport rates from 20 to 100 t km⁻² year⁻¹ in 1941–2000 (Chalov *et al.* , 2018), which can be also attributed to mining impact (Walling & Fang, 2003) or changes due to permafrost thaw (Chalov *et al.* , 2021).

The data presented here shows the hydrochemical patterns of different waters in an environment shaped by permafrost seasonal and long-term changes. The ionic composition of all sampled waters is likely impacted by both suprapermafrost waters and an inflow of deeper, intra- and subpermafrost waters; especially the permafrost creeks P1 and P2 are likely connected to unfrozen groundwater (Cochand *et al.* , 2019).

Among the studied samples, the permafrost creeks differ from river waters by the high content of DOC, major cations and anions, and selected metals and metalloids, including heavy metals. The pathways of OC transport and transformation in Siberian freshwater have been thoroughly analysed recently, e.g. by Wild *et al.* (2019), Mann *et al.* (2022), or Jong *et al.* , (2022). Mann *et al.*(2022) stated that permafrost-derived OC additions will significantly enhance inland OC turnover over the upcoming decades, however the fate of OC is uncertain due to additional transformation factors (Keskitalo *et al.* , 2022). In the large rivers, OC occurs mainly as DOC: for Kolyma, the dissolved share has been calculated by Mann *et al.*(2022) as 80%. Similar values are reported by others (Jong *et al.* , 2022; Keskitalo *et al.* , 2022). Keskitalo *et al.*(2022) have concluded, based on isotopic evidence, that the smaller fraction by mass, the POC, is more affected by the legacy Yedoma-derived OC, than is DOC. Similarly, Wild *et al.* (2019) claim that POC in the large Siberian rivers may originate from the direct erosion of the old Yedoma layers, although they also estimate the legacy OC share in the DOC and POC fractions in the Kolyma to be approximately equal. Bröder *et al.* (2020) remarks that Kolyma transports more suspended POC at higher discharges, and both the total POC and legacy POC concentrations are higher there than in a small stream (the average POC ages in Kolyma and a small stream were estimated at $\sim 2,840$ and ~ 590 years, respectively). These claims are supported by Jong *et al.* (2022), who observed an increased contribution of POC in the TOC transport in large rivers and connected it to the increased direct erosion of the river banks, while a smaller stream exhibited a higher share of DOC. Therefore, the POC in Kolyma likely originates from recent vegetation and old permafrost erosion combined. Mann *et al.* (2022) suggest also that the OC flux and total export will rapidly increase due to climate change and permafrost degradation.

In our research, the DOC concentration in a permafrost ice sample amounted to 9.13 mg L⁻¹ and it was approximately 11 times less than the concentrations in the creeks draining the permafrost cliff. Similar DOC values of 154–336 mg L⁻¹ and 103.4 mg L⁻¹, for creeks draining the permafrost cliff at Duvanny Yar, were obtained by Vonk *et al.* (2013) and Jong *et al.* (2022), respectively, and the concentrations of POC in the same samples amounted to 6700–9240 mg L⁻¹, eclipsing the DOC contribution. (This is also consistent with the additionally sampled POC in P1 and P2 samples, amounting to 8500 and 12000 mg L⁻¹, respectively – methods are reported in the *Supp. Mat. 1.*) Conversely, Jong *et al.* (2022) obtained DOC concentrations (2.76 to 4.97 mg L⁻¹) at approximately double the POC concentrations (1.49 to 2.73 mg L⁻¹) for Kolyma below Duvanny Yar, and similar results for Maly and Bolshoy Anyui (3.16–4.43 mg L⁻¹ and 1.29–1.7 mg L⁻¹, respectively). In our research, thermokarst lakes were studied also, with DOC concentrations similar to a small stream studied by Jong *et al.* (2022), representing soil leaching and active layer drainage ([DOC] = 21.5 mg L⁻¹). The legacy DOC from permafrost can be approximated by the DOC concentration in permafrost ice (9.13 mg L⁻¹), yet the extra 90% of DOC in permafrost creeks may originate both from permafrost active layer (i.e. relatively recent atmospheric deposition and microbial processes) and the exclusion of various organic compounds during groundwater freeze. POC from the ice may also be a source of DOC in thaw waters. The cluster analysis of our data has shown similarities in the water chemistry between the permafrost ice sample (P3), the bottom layer of water in Lake 2 and a sample from Kolyma below Duvanny Yar (K31, sampled mid-depth away from the cliff side, where the main river current flows), which

suggests the influence of legacy permafrost thaw upon the Kolyma river in this cross section. At the same time, the connection between the other lake samples and the samples from the permafrost creeks suggests a general permafrost waters influence over the lake waters, although it is probably a combined influence of the active layer drainage and deeper talik-type waters.

In the collected permafrost ice, a contrastingly high level of aluminium concentration has been noted as compared to the other samples; a relatively high concentration of Al was also found in the permafrost creeks and the sampled lakes. Aluminium co-occurs with K^+ , Be, but also with Co and As, frequently classified as heavy metals. Arsenic occurred at elevated (against other samples) concentrations in the lake bottom waters of this study. In the lake waters, permafrost creeks and permafrost ice, we found also elevated concentrations of other heavy metals (Co, Mn, Ni, Zn, Cu and Sb). Zinc, copper and cadmium showed elevated values also in the Kolyma, while the bottom layer waters of the thermokarst Lake 2 exhibited also a very high concentration of Pb. Monhonval *et al.* (2021) characterised the chemical composition of Yedoma waters, by exploring the mineral element stock in sediments of the Yedoma. They found a relatively high concentration for Si, followed by Al, Fe, K, Ca, Ti, Mn, Zr, Sr, and Zn. Moreover, the stock of Al and Fe (598 +- 213 and 288 +-104 Gt) was at the same order of magnitude as the OC stock (327–466 Gt). Our surface water and ice samples from the Kolyma watershed exhibited similarly high concentrations of Si and Fe, as well as Al. The cluster analysis of all the collected samples shows that in cluster C3, the elements Si and Fe were grouped together with Ni and Mn (Figure 6a). However, in river waters they correlated with Zn, Sb, Cu, V, Co, As, and DOC (cluster c1, Figure 7). Both clusters may be connected to the suprapermafrost waters of the active layer, which are flowing intensely into the thermokarst lakes and rivers. Ji *et al.* (2021) studied elements in permafrost soils and concluded that Mn, Ca, Mg, Al, and Ti showed the highest mobility from soil to suprapermafrost water and further into the ponds and flowing waters. Furthermore, they considered Mn a proxy for predicting the processes occurring in the active layer during summer-autumn thaw. Conversely, the long-term research in the Yukon River basin (1982-2014), underlain by discontinuous permafrost, shows a relationship between the deepening of permafrost active layer and significant increases in the Ca, Mg, and Na annual flux in the Yukon River and its tributary Tanana, and in the SO_4 and P annual flux in the Yukon (Toohey *et al.* , 2016). The authors described increased active layer expansion, weathering, and sulfide oxidation due to permafrost degradation throughout the studied basin. Frey & McClelland (2009) forecast also a significant increase in the concentrations of major ions due to permafrost degradation and lowering water tables (except for nitrate in Siberia). In the studied samples from the Kolyma watershed, clusters C5 and c3 (in the all sample and river sample analysis, respectively; Figure 6a, Figure 7) indicate the likely influence of rock weathering on water composition. The visible division within the c3 cluster into c3a (Sr, Se, K^+ , Mg^{2+} , Ca^{2+} and SO_4^{2-}) and c3b (Cl^- , Na^+ and F^-) may represent two separate water supply factors, namely the shallow and deep groundwater flow (Douglas *et al.* , 2013). An extra contribution to the total sulphate load in the rivers may also result from the wet deposition connected to wildfires, which have influenced considerably the deposition of sulphur (and nitrogen) compounds in the regions of Siberia and the Russian Far East (Berezin *et al.* , 2013). On the other hand, the lower contribution of Ca^{2+} in thermokarst lake waters may result, according to Monhonval *et al.* (2021), from the leaching of soluble elements such as Ca during former thaw periods.

In this study, mercury was found only in permafrost creeks, permafrost ice and in the Maly Anyui. Recent research has shown that Hg may be released from continental permafrost with climate-change-induced thaw, and there are very different quantitative estimates of Hg fluxes connected to various local sources (permafrost is considered one source among the many; Campeau *et al.* , 2022; Ci *et al.* , 2020; Muet *et al.* , 2020; Schuster *et al.* , 2018). Schuster *et al.* (2018) estimated that the entire Northern Hemisphere permafrost area contains 1,656 +- 962 Gg Hg, of which 793 +- 461 Gg Hg (~47%) is frozen in permafrost. Except in permafrost ice, our samples may contain mercury of various origin, both from permafrost thaw and from atmospheric deposition (Schuster *et al.* , 2018), and in the case of Maly Anyui it may also be connected to mining. (Gold mining occurs in parts of both the Maly and Bolshoy Anyui catchments, yet higher production comes from around the Maly Anyui tributary Karalveem River). However, the low Hg concentrations (<LOD) in the other collected samples (from Kolyma, Omolon and the lakes) indicate that any atmospheric sources of Hg would likely be only local and periodic (e.g., forest fires) (Francisco Lopez *et al.* , 2022). Furthermore, it

cannot be excluded that most Hg in the analysed samples occurred in the particulate form, which has not been investigated here. Lim *et al.* (2019), who have analysed the POC and Hg fluxes in the rivers of various permafrost zones, indicate minimal particulate Hg export at the sporadic to discontinuous permafrost zone. According to these authors, the current climate warming, the northward shift of permafrost boundaries and the increasing active layer depth in Western Siberia, may result in an enhanced particulate Hg export by small rivers to the Arctic Ocean by a factor of two over the next 10-50 years. The possible origin of the Hg may be also connected to mining areas (both abandoned and active) distributed over Maly Anyui river.

Besides mercury, also As and Cd are heavy metals sometimes mentioned as posing a new hazard due to permafrost thaw (Zhang *et al.* , 2021). In this study, a potential source of those is the erosion of a permafrost cliff, given the significant enrichment of As and Cd in permafrost ice, the extremely high EF in permafrost creeks, and very high to extremely high EF in the deep waters of thermokarst lakes (Table S4, *Suppl. Mat. 1*). The supply of Cd may be connected to the drainage of mixed suprapermfrost water, which may include atmospheric deposition, and deeper water both. With the active layer deepening, atmospheric pollutants deposited in the past, which have been excluded from the freeze-thaw cycle for a time (Ji *et al.* , 2021), may be remobilised (Edwards *et al.* , 2021; Li *et al.* , 2020; Lim *et al.* , 2019; Rubino *et al.* , 2016). The notable increase in Cu, Ni, Pb and Zn concentrations in deep lake waters indicate the likely source of these elements in permafrost thaw, talik water, or enhanced mobility of suprapermfrost water eluting them from soil. Importantly, it is not only in the Lake 1 near the Cherskii research station and the settlement which experienced the elevated concentrations of these metals in the bottom waters, but also in the further from any human activity Lake 2, showing that such contamination is probably irrelevant of local infrastructure.

In the studied freshwaters, it was evident that thermokarst lakes form at least temporary traps for heavy metals connected to one or several types of permafrost influence. Thermokarst lakes form one of the more dynamic elements of the continental permafrost landscape, and their mass emergence is among the more frequently observed impacts of climate change in the Northern Hemisphere (in't Zandt *et al.* , 2020; Karlsson *et al.* , 2012; Plug *et al.* , 2008), including the Kolyma region (Veremeeva *et al.* , 2021). Due to the dynamically increasing number of thermokarst lakes, and their predicted drainage with the advancing climate change and deepening active layer, the sedimentation in these lakes and the biogeochemical processes happening in them (in't Zandt *et al.* , 2020) will likely be of high importance in studies of continental permafrost areas.

5. CONCLUSIONS

In our study of the dissolved inorganic chemistry in the lower Kolyma basin, we found that the ionic HCO₃-Ca-Mg water type was prevalent (representing both lakes and permafrost ice), and the river and permafrost creek waters had also a significant admixture of sulphate. The highest concentrations of DOC (9.13-127 mg/L) were found in permafrost ice, permafrost creeks and thermokarst lakes, i.e. the water bodies connected to permafrost thaw. Among the collected water samples, a few heavy metals were detected at higher concentrations in permafrost-related samples than elsewhere, i.e. As, Cd, Co, Fe, Mn, Ni, and V. The occasionally detected Cr, Hg, Pb and Ti were also typically associated with the permafrost-related origin of a sample. Mercury occurred also at a relatively high concentration in the Maly Anyui tributary of Kolyma. The highest concentrations of most of the studied elements were found in the lake bottom waters, suggesting that thermokarst lakes act as local traps for elements, including heavy metals. Further evidence for the origin of these metals could be provided in the future through sampling lake bottom sediments as well.

The impact of changes in permafrost regions, occurring due to climate change, need to be considered with respect to both the remobilisation from older permafrost (of organic carbon and other chemical components) and the interference with newly deposited anthropogenic contaminants. Such impacts are likely to be complex and modified by the local sedimentation processes in the local watercourses and lakes. The further forecasted climate change may result in the formation of new flow pathways for dissolved chemicals migrating between supra-, intra- and subpermafrost waters. Further research into the concentration of dissolved and particulate phases in permafrost thaw and active layer waters is warranted to diminish the uncertainties related to this field of knowledge or to estimate the total load of e.g. heavy metals in the permafrost regions, available to remobilisation.

Funding

This research was funded by INTERACT, H2020-EU.1.4.1.2. (*PollAct*, grant no. 730938) and by the Project Supporting Maintenance of Research Potential at Kazimierz Wielki University. K.K.'s fieldwork was supported by similar Research Potential Maintenance funds of the Gdansk University of Technology. S.Ch. and V.E. acknowledge the support of RSF for fieldwork (project 21-17-00181).

Acknowledgements

We are grateful to F. Pawlak and B. Knoebelsdorf for their aid in sample preparation, and to J. Potapowicz for EF calculations. Special thanks to M. Szopińska and the North-East Science Station for help during fieldwork.

Conflict of Interest Statement

The authors declare no conflict of interest.

Data Availability Statement

The data is currently under restricted access in the Zenodo Open Data repository: <https://zenodo.org/record/7452043>, to be released upon manuscript publication.

References

- Abramov A, Davydov S, Ivashchenko A, Karelin D, Kholodov A, Kraev G, Lupachev A, Maslakov A, Ostroumov V, Rivkina E, Shmelev D, Sorokovikov V, Tregubov O, Veremeeva A, Zamolodchikov D, Zimov S. 2021. Two decades of active layer thickness monitoring in northeastern Asia. *Polar Geography* **44** : 186–202. DOI: 10.1080/1088937X.2019.1648581
- Berezin E V., Konovalov IB, Gromov SA, Beekmann M, Schulze E-D. 2013. The model study of the wildfire impact on the spatial distribution of deposition of sulfur and nitrogen compounds in Siberia. *Russian Meteorology and Hydrology* **38** : 750–758. DOI: 10.3103/S1068373913110046
- Bröder L, Davydova A, Davydov S, Zimov N, Haghypour N, Eglinton TI, Vonk JE. 2020. Particulate Organic Matter Dynamics in a Permafrost Headwater Stream and the Kolyma River Mainstem. *Journal of Geophysical Research: Biogeosciences* **125** . DOI: 10.1029/2019JG005511
- Brubaker M, Chavan P, Berner PEJ, Black M, Warren J. 2012. *Climate Change in Selawik, Alaska* .
- Campeau A, Eklöf K, Soerensen AL, Åkerblom S, Yuan S, Hintelmann H, Bieroza M, Köhler S, Zdanowicz C. 2022. Sources of riverine mercury across the Mackenzie River Basin; inferences from a combined Hg C isotopes and optical properties approach. *Science of The Total Environment* **806** : 150808. DOI: 10.1016/j.scitotenv.2021.150808
- Chalov S, Moreido V, Ivanov V, Chalova A. 2022. Assessing suspended sediment fluxes with acoustic Doppler current profilers: case study from large rivers in Russia. *Big Earth Data* 1–23. DOI: 10.1080/20964471.2022.2116834
- Chalov S, Prokopeva K, Habel M. 2021. North to South Variations in the Suspended Sediment Transport Budget within Large Siberian River Deltas Revealed by Remote Sensing Data. *Remote Sensing* **13** : 4549. DOI: 10.3390/rs13224549
- Chalov SR, Liu S, Chalov RS, Chalova ER, Chernov A V., Promakhova E V., Berkovitch KM, Chalova AS, Zavadsky AS, Mikhailova N. 2018. Environmental and human impacts on sediment transport of the largest Asian rivers of Russia and China. *Environmental Earth Sciences* **77** : 274. DOI: 10.1007/s12665-018-7448-9
- Ci Z, Peng F, Xue X, Zhang X. 2020. Permafrost Thaw Dominates Mercury Emission in Tibetan Thermokarst Ponds. *Environmental Science & Technology* **54** : 5456–5466. DOI: 10.1021/acs.est.9b06712

- Cochand M, Molson J, Lemieux J. 2019. Groundwater hydrogeochemistry in permafrost regions. *Permafrost and Periglacial Processes* **30** : 90–103. DOI: 10.1002/ppp.1998
- Douglas TA, Blum JD, Guo L, Keller K, Gleason JD. 2013. Hydrogeochemistry of seasonal flow regimes in the Chena River, a subarctic watershed draining discontinuous permafrost in interior Alaska (USA). *Chemical Geology* **335** : 48–62. DOI: 10.1016/j.chemgeo.2012.10.045
- Dzhamalov RG, Safronova TI. 2018. Effect of Permafrost Rocks on Water Resources Formation in Eastern Siberia: Case Study of Some Rivers in Eastern Siberia. *Water Resources* **45** : 455–465. DOI: 10.1134/S0097807818040097
- Edwards BA, Kushner DS, Outridge PM, Wang F. 2021. Fifty years of volcanic mercury emission research: Knowledge gaps and future directions. *Science of The Total Environment* **757** : 143800. DOI: 10.1016/j.scitotenv.2020.143800
- Francisco López A, Heckenauer Barrón EG, Bello Bugallo PM. 2022. Contribution to understanding the influence of fires on the mercury cycle: Systematic review, dynamic modelling and application to sustainable hypothetical scenarios. *Environmental Monitoring and Assessment* **194** : 707. DOI: 10.1007/s10661-022-10208-3
- Frey KE, McClelland JW. 2009. Impacts of permafrost degradation on arctic river biogeochemistry. **182** : 169–182. DOI: 10.1002/hyp
- Grigoriev MN, Kunitsky VV, Chzhan RV, Shepelev VV. 2009. On the variation in geocryological, landscape and hydrological conditions in the Arctic zone of East Siberia in connection with climate warming. *Geography and Natural Resources* **30** : 101–106. DOI: 10.1016/j.gnr.2009.06.002
- Grosse G, Goetz S, McGuire AD, Romanovsky VE, Schuur EAG. 2016. Changing permafrost in a warming world and feedbacks to the Earth system. *Environmental Research Letters* **11** : 040201. DOI: 10.1088/1748-9326/11/4/040201
- Gunnarsdóttir MJ, Gararsson SM, Andradóttir HÓ, Schiöth A. 2019. Áhrif Loftlagsbreytinga Á Vatnsveitur Og Vatnsgæi Á Íslandi – Áhættuættir Og Agerir. *Icelandic Journal of Engineering* **25** : 5–19. DOI: 10.33112/ije.25.5
- Günther F, Overduin PP, Yakshina IA, Opel T, Baranskaya A V., Grigoriev MN. 2015. Observing Muostakh disappear: permafrost thaw subsidence and erosion of a ground-ice-rich island in response to arctic summer warming and sea ice reduction. *The Cryosphere* **9** : 151–178. DOI: 10.5194/tc-9-151-2015
- Holmes RM, McClelland JW, Peterson BJ, Tank SE, Bulygina E, Eglinton TI, Gordeev V V, Gurtovaya TY, Raymond PA, Repeta DJ, Staples R, Striegl RG, Zhulidov A V, Zimov SA. 2012. Seasonal and Annual Fluxes of Nutrients and Organic Matter from Large Rivers to the Arctic Ocean and Surrounding Seas. 369–382. DOI: 10.1007/s12237-011-9386-6
- in 't Zandt MH, Liebner S, Welte CU. 2020. Roles of Thermokarst Lakes in a Warming World. *Trends in Microbiology* **28** : 769–779. DOI: 10.1016/j.tim.2020.04.002
- Ji X, Abakumov E, Polyakov V, Xie X. 2021. Mobilization of Geochemical Elements to Surface Water in the Active Layer of Permafrost in the Russian Arctic. *Water Resources Research* **57** . DOI: 10.1029/2020WR028269
- Jong D, Bröder L, Tesi T, Keskitalo K, Zimov N, Davydova A, Pika P, Haghypour N, Eglinton T, Vonk J. 2022. Contrasts in dissolved, particulate and sedimentary organic carbon from the Kolyma River to the East Siberian Shelf. *preprint (EGUsphere)* . DOI: 10.5194/egusphere-2022-516
- Karlsson JM, Lyon SW, Destouni G. 2012. Thermokarst lake, hydrological flow and water balance indicators of permafrost change in Western Siberia. *Journal of Hydrology* **464 –465** : 459–466. DOI: 10.1016/j.jhydrol.2012.07.037

- Keskitalo KH, Bröder L, Jong D, Zimov N, Davydova A, Davydov S, Tesi T, Mann PJ, Haghypour N, Eglinton TI, Vonk JE. 2022. Seasonal variability in particulate organic carbon degradation in the Kolyma River, Siberia. *Environmental Research Letters* **17** : 034007. DOI: 10.1088/1748-9326/ac4f8d
- Kokelj S V., Lacelle D, Lantz TC, Tunnicliffe J, Malone L, Clark ID, Chin KS. 2013. Thawing of massive ground ice in mega slumps drives increases in stream sediment and solute flux across a range of watershed scales. *Journal of Geophysical Research: Earth Surface* **118** : 681–692. DOI: 10.1002/jgrf.20063
- Kosek K, Koziol K, Luczkiewicz A, Jankowska K, Chmiel S, Polkowska Ż. 2019. Environmental characteristics of a tundra river system in Svalbard. Part 2: Chemical stress factors. *Science of the Total Environment* **653** . DOI: 10.1016/j.scitotenv.2018.11.012
- Kuchmenko E V, Moloznikova Y V, Netsvetaeva OG, Kobeleva NA, Khodzher T V. 2002. Comparison of Experimental and Calculated Data on Ion Composition of Precipitation in the South of East Siberia. In: Barnes I (ed) *Global Atmospheric Change and its Impact on Regional Air Quality* . Springer Netherlands: Dordrecht, 223–228. DOI: 10.1007/978-94-010-0082-6_34
- Lehmann-Konera S, Franczak Ł, Kociuba W, Szumińska D, Chmiel S, Polkowska Ż. 2018. Comparison of hydrochemistry and organic compound transport in two non-glaciated high Arctic catchments with a permafrost regime (Bellsund Fjord, Spitsbergen). *Science of The Total Environment* **613–614** : 1037–1047. DOI: 10.1016/j.scitotenv.2017.09.064
- Li Y, Zang S, Zhang K, Sun D, Sun L. 2020. Occurrence, sources and potential risks of polycyclic aromatic hydrocarbons in a permafrost soil core, northeast China. *Ecotoxicology* . DOI: 10.1007/s10646-020-02285-2
- Lim AG, Sonke JE, Krickov I V, Manasyrov RM, Loiko S V, Pokrovsky OS. 2019. Enhanced particulate Hg export at the permafrost boundary, western Siberia. *Environmental Pollution* **254** : 113083. DOI: <https://doi.org/10.1016/j.envpol.2019.113083>
- Mann PJ, Davydova A, Zimov N, Spencer RGM, Davydov S, Bulygina E, Zimov S, Holmes RM. 2012. Controls on the composition and lability of dissolved organic matter in Siberia’s Kolyma River basin. *Journal of Geophysical Research: Biogeosciences* **117** . DOI: 10.1029/2011JG001798
- Mann PJ, Strauss J, Palmtag J, Dowdy K, Ogneva O, Fuchs M, Bedington M, Torres R, Polimene L, Overduin P, Mollenhauer G, Grosse G, Rachold V, Sobczak W V., Spencer RGM, Juhls B. 2022. Degrading permafrost river catchments and their impact on Arctic Ocean nearshore processes. *Ambio* **51** : 439–455. DOI: 10.1007/s13280-021-01666-z
- Monhonval A, Mauclet E, Pereira B, Vandeuren A, Strauss J, Grosse G, Schirrmeister L, Fuchs M, Kuhry P, Opfergelt S. 2021. Mineral Element Stocks in the Yedoma Domain: A Novel Method Applied to Ice-Rich Permafrost Regions. *Frontiers in Earth Science* **9** . DOI: 10.3389/feart.2021.703304
- Morgenstern A, Overduin PP, Günther F, Stettner S, Ramage J, Schirrmeister L, Grigoriev MN, Grosse G. 2021. Thermo-erosional valleys in Siberian ice-rich permafrost. *Permafrost and Periglacial Processes* **32** : 59–75. DOI: 10.1002/ppp.2087
- Mu C, Schuster PF, Abbott BW, Kang S, Guo J, Sun S, Wu Q, Zhang T. 2020. Permafrost degradation enhances the risk of mercury release on Qinghai-Tibetan Plateau. *Science of The Total Environment* **708** : 135127. DOI: 10.1016/j.scitotenv.2019.135127
- Nitzbon J, Westermann S, Langer M, Martin LCP, Strauss J, Laboor S, Boike J. 2020. Fast response of cold ice-rich permafrost in northeast Siberia to a warming climate. *Nature Communications* **11** : 2201. DOI: 10.1038/s41467-020-15725-8
- Nitze I, Grosse G, Jones B, Arp C, Ulrich M, Fedorov A, Veremeeva A. 2017. Landsat-Based Trend Analysis of Lake Dynamics across Northern Permafrost Regions. *Remote Sensing* **9** : 640. DOI: 10.3390/rs9070640

- Overland J. WJ. K V. 2017. Trends and feedbacks. In: Symon C. (ed) *Snow, Water, Ice and Permafrost in the Arctic (SWIPA) 2017* . Arctic Monitoring and Assessment Programme (AMAP): Oslo, Norway, 9–24
- Overland JE, Wang M, Walsh JE, Stroeve JC. 2014. Future Arctic climate changes: Adaptation and mitigation time scales. *Earth's Future* **2** : 68–74. DOI: 10.1002/2013EF000162
- Plug LJ, Walls C, Scott BM. 2008. Tundra lake changes from 1978 to 2001 on the Tuktoyaktuk Peninsula, western Canadian Arctic. *Geophysical Research Letters* **35** : L03502. DOI: 10.1029/2007GL032303
- Potapowicz J, Szumińska D, Szopińska M, Polkowska Ż. 2019. The influence of global climate change on the environmental fate of anthropogenic pollution released from the permafrost: Part I. Case study of Antarctica. *Science of the Total Environment* . DOI: 10.1016/j.scitotenv.2018.09.168
- Ran Y, Li X, Cheng G, Che J, Aalto J, Karjalainen O, Hjort J, Luoto M, Jin H, Obu J, Hori M, Yu Q, Chang X. 2022. New high-resolution estimates of the permafrost thermal state and hydrothermal conditions over the Northern Hemisphere. *Earth System Science Data* **14** : 865–884. DOI: 10.5194/essd-14-865-2022
- Rubino M, D'Onofrio A, Seki O, Bendle JA. 2016. Ice-core records of biomass burning. *The Anthropocene Review* **3** : 140–162. DOI: 10.1177/2053019615605117
- Rudy ACA, Lamoureux SF, Kokelj S V., Smith IR, England JH. 2017. Accelerating Thermokarst Transforms Ice-Cored Terrain Triggering a Downstream Cascade to the Ocean. *Geophysical Research Letters* **44** : 11,080–11,087. DOI: 10.1002/2017GL074912
- Sakai T, Matsunaga T, Maksyutov S, Gotovtsev S, Gagarin L, Hiyama T, Yamaguchi Y. 2016. Climate-Induced Extreme Hydrologic Events in the Arctic. *Remote Sensing* **8** : 971. DOI: 10.3390/rs8110971
- Schuster PF, Schaefer KM, Aiken GR, Antweiler RC, Dewild JF, Gryziec JD, Gusmeroli A, Hugelius G, Jafarov E, Krabbenhoft DP, Liu L, Herman-Mercer N, Mu C, Roth DA, Schaefer T, Striegl RG, Wickland KP, Zhang T. 2018. Permafrost Stores a Globally Significant Amount of Mercury. *Geophysical Research Letters* **45** : 1463–1471. DOI: 10.1002/2017GL075571
- Smith SL, O'Neill HB, Isaksen K, Noetzli J, Romanovsky VE. 2022. The changing thermal state of permafrost. *Nature Reviews Earth & Environment* **3** : 10–23. DOI: 10.1038/s43017-021-00240-1
- Stepanenko VM, Machul'skaya EE, Glagolev M V., Lykossov VN. 2011. Numerical modeling of methane emissions from lakes in the permafrost zone. *Izvestiya, Atmospheric and Oceanic Physics* **47** : 252–264. DOI: 10.1134/S0001433811020113
- Strauss J, Laboor S, Schirrmeister L, Fedorov AN, Fortier D, Froese D, Fuchs M, Günther F, Grigoriev M, Harden J, Hugelius G, Jongejans LL, Kanevskiy M, Kholodov A, Kunitsky V, Kraev G, Lozhkin A, Rivkina E, Shur Y, Siegert C, Spektor V, Streletskaya I, Ulrich M, Vartanyan S, Veremeeva A, Anthony KW, Wetterich S, Zimov N, Grosse G. 2021. Circum-Arctic Map of the Yedoma Permafrost Domain. *Frontiers in Earth Science* **9** . DOI: 10.3389/feart.2021.758360
- Streletskiy D. 2021. Permafrost degradation. *Snow and Ice-Related Hazards, Risks, and Disasters* . Elsevier, 297–322. DOI: 10.1016/B978-0-12-817129-5.00021-4
- Streletskiy DA, Maslakov AA, Streletskaya ID, Nelson FE. 2021. Permafrost Regions In Transition: Introduction. *GEOGRAPHY, ENVIRONMENT, SUSTAINABILITY* **14** : 6–8. DOI: 10.24057/2071-9388-2021-081
- Streletskiy DA, Sherstiukov AB, Frauenfeld OW, Nelson FE. 2015. Changes in the 1963–2013 shallow ground thermal regime in Russian permafrost regions. *Environmental Research Letters* **10** : 125005. DOI: 10.1088/1748-9326/10/12/125005
- Suzuki K, Park H, Makarieva O, Kanamori H, Hori M, Matsuo K, Matsumura S, Nesterova N, Hiyama T. 2021. Effect of Permafrost Thawing on Discharge of the Kolyma River, Northeastern Siberia. *Remote Sensing* **13** : 4389. DOI: 10.3390/rs13214389

- Szopińska M, Dymerski T, Polkowska Ż, Szumińska D, Wolska L. 2016. The chemistry of river–lake systems in the context of permafrost occurrence (Mongolia, Valley of the Lakes) Part II. Spatial trends and possible sources of organic composition. *Sedimentary Geology* **340** : 84–95. DOI: 10.1016/j.sedgeo.2016.03.001
- Tananaev N, Isaev V, Sergeev D, Kotov P, Komarov O. 2021. Hydrological Connectivity in a Permafrost Tundra Landscape near Vorkuta, North-European Arctic Russia. *Hydrology* **8** : 106. DOI: 10.3390/hydrology8030106
- Tananaev N, Lotsari E. 2022. Defrosting northern catchments: Fluvial effects of permafrost degradation. *Earth-Science Reviews* **228** : 103996. DOI: 10.1016/j.earscirev.2022.103996
- Taylor SR. 1964. Abundance of chemical elements in the continental crust: a new table. *Geochimica et Cosmochimica Acta* **28** : 1273–1285. DOI: 10.1016/0016-7037(64)90129-2
- Teufel B, Sushama L. 2019. Abrupt changes across the Arctic permafrost region endanger northern development. *Nature Climate Change* **9** : 858–862. DOI: 10.1038/s41558-019-0614-6
- Toohy RC, Herman-Mercer NM, Schuster PF, Mutter EA, Koch JC. 2016. Multidecadal increases in the Yukon River Basin of chemical fluxes as indicators of changing flowpaths, groundwater, and permafrost. *Geophysical Research Letters* **43** : 12,120–12,130. DOI: 10.1002/2016GL070817
- Veremeeva A, Nitze I, Günther F, Grosse G, Rivkina E. 2021. Geomorphological and Climatic Drivers of Thermokarst Lake Area Increase Trend (1999–2018) in the Kolyma Lowland Yedoma Region, North-Eastern Siberia. *Remote Sensing* **13** : 178. DOI: 10.3390/rs13020178
- Viers J, Dupré B, Gaillardet J. 2009. Chemical composition of suspended sediments in World Rivers: New insights from a new database. *Science of The Total Environment* **407** : 853–868. DOI: 10.1016/j.scitotenv.2008.09.053
- Vonk JE, Mann PJ, Davydov S, Davydova A, Spencer RGM, Schade J, Sobczak W V., Zimov N, Zimov S, Bulygina E, Eglinton TI, Holmes RM. 2013. High biolability of ancient permafrost carbon upon thaw. *Geophysical Research Letters* **40** : 2689–2693. DOI: 10.1002/grl.50348
- Vonk JE, Tank SE, Bowden WB, Laurion I, Vincent WF, Alekseychik P, Amyot M, Billet MF, Canário J, Cory RM, Deshpande BN, Helbig M, Jammet M, Karlsson J, Larouche J, MacMillan G, Rautio M, Walter Anthony KM, Wickland KP. 2015. Reviews and syntheses: Effects of permafrost thaw on Arctic aquatic ecosystems. *Biogeosciences* **12** : 7129–7167. DOI: 10.5194/bg-12-7129-2015
- Walling DE, Fang D. 2003. Recent trends in the suspended sediment loads of the world’s rivers. *Global and Planetary Change* **39** : 111–126. DOI: 10.1016/S0921-8181(03)00020-1
- Walter KM, Zimov SA, Chanton JP, Verbyla D, Chapin FS. 2006. Methane bubbling from Siberian thaw lakes as a positive feedback to climate warming. *Nature* **443** : 71–75. DOI: 10.1038/nature05040
- Wang W, Ji X, Abakumov E, Polyakov V, Li G, Wang D. 2022. Assessing Sources and Distribution of Heavy Metals in Environmental Media of the Tibetan Plateau: A Critical Review. *Frontiers in Environmental Science* **10** . DOI: 10.3389/fenvs.2022.874635
- Wild B, Andersson A, Bröder L, Vonk J, Hugelius G, McClelland JW, Song W, Raymond PA, Gustafsson Ö. 2019. Rivers across the Siberian Arctic unearth the patterns of carbon release from thawing permafrost. *Proceedings of the National Academy of Sciences* **116** : 10280–10285. DOI: 10.1073/pnas.1811797116
- Yershov ED, Kondratyeva KA, Loginov IK, Sychev IK. 1991. Geocryological map of Russia and neighbouring Republics, scale 1:2,500,000, 16 sheets [in Russian]. *English translation of map symbols and legends: Williams, P.J., & Warren, I.M.T. (eds. 1999)*
- Zhang S, Yang G, Hou S, Zhang T, Li Z, Du W. 2021. Analysis of heavy metal-related indices in the Eboing permafrost on the Tibetan Plateau. *CATENA* **196** : 104907. DOI: 10.1016/j.catena.2020.104907

